Bandwidth- and Power-Efficient Multicarrier Multiple Access

Pengfei Xia, *Student Member, IEEE*, Shengli Zhou, *Member, IEEE*, and Georgios B. Giannakis, *Fellow, IEEE*

***Abstract*—Orthogonal frequency-division multiple access (OFDMA) gains increasing attention for broadband, high data rate wireless communications. In this paper, we develop a novel unitary precoded (UP) OFDMA scheme that is particularly appealing for the uplink, because it offers high bandwidth efficiency, and constant modulus transmissions for each user. Theoretical analysis of UP-OFDMA with channel coding shows the performance improvement introduced by unitary precoding. It provides useful guidelines for practical system designs, and also quantifies the performance of UP-OFDMA relative to the single-user bound. Simulations confirm that UP-OFDMA improves performance considerably relative to conventional OFDMA.**

***Index Terms*—Constant modulus, diversity, multiple access, orthogonal frequency-division multiplexing (OFDM), unitary precoding (UP).**

I. Introduction

BROADBAND wireless applications require effective handling of intersymbol interference (ISI) that arises when high-rate transmissions propagate through time dispersive (or frequency selective) channels. Using inverse fast Fourier transform (IFFT) and cyclic prefix (CP) insertion at the transmitter, together with CP removal and IFFT processing at the receiver, orthogonal frequency-division multiplexing (OFDM) converts frequency-selective ISI channels into a set of parallel flat fading subchannels, which reduces the equalization complexity considerably. Thanks to its ability to cope with ISI channels, OFDM has found widespread applications in digital subscriber lines (DSL), digital audio/video broadcasting (DAB/DVB), and wireless local area networking (LAN) standards, including IEEE802.11a and Hiperlan/2.

Being OFDM's counterpart for multiuser communications, orthogonal frequency-division multiple access (OFDMA) inherits its attractive features. Originally proposed for cable TV networks [12], it is now being considered for IEEE802.16a [8], ETSI Broadband Radio Access Networks (BRAN) [2], and multiuser satellite communications [20].

In its simplest form, each OFDMA user transmits information symbols using one complex exponential (subcarrier) that retains its orthogonality with other users' subcarriers, even when passing through multipath fading channels. As a result, multiuser interference (MUI) is suppressed deterministically, regardless of the underlying ISI channels. In uplink applications, this one-carrier-per-user access scheme is also power efficient, since each user maintains a constant modulus transmission. However, the performance of OFDMA suffers considerably if the user-specific channel exhibits deep fades (or nulls) at the information-bearing subcarrier. To robustify performance against channel fades, error-control coding and/or frequency hopping are usually employed [12], [25]. On the other hand, multiple subcarriers can be assigned per user to support high data rate applications at the expense of nonconstant modulus signaling, which reduces efficiency of the power amplification stage at the transmitter.

Recently, redundant linear precoding across subcarriers has been proposed in the so-termed generalized multicarrier (GMC)-code-division multiple access (CDMA) [5], [17], which improves performance considerably over conventional OFDMA. However, the redundancy of GMC-CDMA (that is equal to the channel memory) reduces bandwidth efficiency proportional to the channels' delay spread. For those GMC-CDMA transmissions that are nonconstant modulus, power amplifier backoff is also required.

In this paper, we derive a unitary precoded (UP) OFDMA scheme (Section III), that achieves high bandwidth efficiency. Even with multiple subcarriers per user, UP-OFDMA maintains perfectly constant modulus transmissions, and is highly power efficient. To evaluate the improvement introduced by unitary precoding, we carry out theoretical performance analysis of UP-OFDMA with channel coding (Section IV). This analysis discloses substantial advantage of unitary precoding, and quantifies the power savings of UP-OFDMA over conventional OFDMA, when both systems employ identical error-control codes. It also provides useful guidelines for selecting the precoder size in practice, and reveals that UP-OFDMA incurs only a small loss relative to the bound achieved by single-user spread-spectrum transmissions.

Notation: Bold uppercase letters denote matrices, while bold lowercase letters denote column vectors; $\star$ denotes convolution, and $\otimes$ stands for Kronecker product; $(\cdot)^T$ and $(\cdot)^{\mathcal{H}}$ denote transpose and Hermitian transpose, respectively; $\mathbf{0}_{M\times N}$ $(\mathbf{1}_{M\times N})$ denotes an all-zero (all-one) matrix with size $M \times N$; $\mathbf{I}_K$ denotes the $K \times K$ identity matrix, and $\mathbf{F}_N$ stands for the

Paper approved by C. Tellambura, the Editor for Modulation and Signal Design of the IEEE Communications Society. Manuscript received May 31, 2002; revised May 27, 2003. This work was sponsored by the Communications and Networks Consortium, sponsored by the U. S. Army Research Laboratory under the Collaborative Technology Alliance Program, Cooperative Agreement DAAD19-01-2-0011. The U. S. Government is authorized to reproduce and distribute reprints for Government purposes notwithstanding any copyright notation thereon. This work was also supported by the National Science Foundation under Grant 01-0516. This paper was presented in part at the IEEE Wireless Communications and Networking Conference, New Orleans, LA, March 16-20, 2003.

P. Xia and G. B. Giannakis are with the Department of Electrical and Computer Engineering, University of Minnesota, Minneapolis, MN 55455 USA (e-mail: pfxia@ece.umn.edu; georgios@ece.umn.edu).

S. Zhou was with the Department of Electrical and Computer Engineering, University of Minnesota, Minneapolis, MN 55455 USA. He is now with the Department of Electrical and Computer Engineering, University of Connecticut, Storrs, CT 06269 USA (e-mail: shengli@engr.uconn.edu).

Digital Object Identifier 10.1109/TCOMM.2003.819198

$N \times N$ FFT matrix with its $(p+1, q+1)$st entry given by $(1/\sqrt{N})\exp(-j2\pi pq/N)$, $\forall\ p, q\ \in\ [0, N-1]$; finally, $[\cdot]_p$ denotes the $(p+1)$st entry of a vector, and $[\cdot]_{p,q}$ denotes the $(p+1, q+1)$st entry of a matrix.

II. Unifying System Model

A. Channel Model

We focus on quasi-synchronous (QS) uplink transmissions over wireless channels, where mobile users follow the base station's pilot signal, to ensure that their relative asynchronism is down to a few chips [1]. Let $g_u(t) = \sum_{l=0}^{\tilde{L}_u} \alpha_{u,l}\delta(t-\tau_{u,l})$ denote the continuous time multipath channel for user u, which consists of $\tilde{L}_u + 1$ paths, each having its own fading coefficient $\alpha_{u,l}$, and distinct delay $\tau_{u,l}$. Denote with $\varphi_u(t)$ and $\bar{\varphi}_u(t)$ the transmit and receive filters for user u, respectively. The discrete-time baseband-equivalent channel corresponding to user u can be modeled as a finite impulse response (FIR) filter [10], with channel tap vector $\mathbf{h}_u := [h_u(0), h_u(1), \ldots, h_u(L)]^T$, where L is an upper bound on the channel orders of all users. The chip rate $(1/T_c)$ sampled FIR channel for user u is thus

$$h_u(n) := (\varphi_u(t) \star g_u(t) \star \bar{\varphi}_u(t))|_{t=nT_c}, \quad n \in [0, L]. \quad (1)$$

If $\tau_{\max,a}$ denotes the maximum asynchronism among users, and $\tau_{\max,s}$ stands for the maximum delay spread among all users' channels, the channel order L satisfies

$$L \geq \left\lceil \frac{\tau_{ax,a} + \tau_{ax,s}}{T_c} \right\rceil.$$

Regardless of the number of physical paths $(\tilde{L}_u)$, the discrete time channels end up with no more than $L+1$ nonzero taps. In a rich scattering environment (large $\tilde{L}_u$), the channel taps $\{h_u(l)\}_{l=0}^{L}$ are approximately uncorrelated. But for sparse channels with only a few physical paths (small $\tilde{L}_u$) and relatively long delays (large $\tau_{u,l}$), these $L+1$ channel taps in $\mathbf{h}_u$ will be highly correlated, with $\tilde{L}_u + 1$ degrees of freedom that are determined by the physical channel. Our UP-OFDMA scheme will be suitable for both rich-scattering and sparse channels.

B. Single-User OFDM

In OFDM block transmissions, the information symbols $s(n)$ are first parsed into blocks

$$\mathbf{s}(i) := [s(iN), \ldots, s(iN+N-1)]^T$$

of length N. The IFFT is then taken to form blocks $\mathbf{F}_N^{\mathcal{H}}\mathbf{s}(i)$. Let the $(n+1)$st column of $\mathbf{F}_N^{\mathcal{H}}$ be

$$\mathbf{f}_n := \left(\frac{1}{\sqrt{N}}\right)\left[e^{j0}, e^{j2\pi n/N}, \ldots, e^{[j2\pi n(N-1)/N]}\right]^T$$

where vectors $\{\mathbf{f}_n\}_{n=0}^{N-1}$ denote the N digital subcarriers. Each information symbol rides on a distinct subcarrier, and the resulting chip sequence is

$$\mathbf{x}(i) = \sum_{n=0}^{N-1} \mathbf{f}_n s(iN+n).$$

To avoid interblock interference, a CP of length L is inserted at the transmitter, and removed at the receiver. CP insertion and removal convert linear convolution to circular convolution. Each subcarrier is an eigen function of the resulting circulant FIR channel, and thus preserves its shape after passing through the channel. The received block, after CP removal, can be written as (see e.g., [17])

$$\mathbf{y}(i) = \sum_{n=0}^{N-1} H(\rho_n)\mathbf{f}_n s(iN+n) + \bar{\mathbf{w}}(i) \quad (2)$$

where $\rho_n := \exp(j2\pi n/N)$ is the frequency of subcarrier $\mathbf{f}_n$, $H(\rho_n)$ is the channel frequency response $H(z) := \sum_{l=0}^{L} h(l)z^{-l}$ evaluated at ρ_n, and $\bar{\mathbf{w}}(i)$ is the additive white Gaussian noise (AWGN) with variance σ_w^2. Each information symbol can then be separated by exploiting the orthogonality among subcarriers to obtain

$$r_n(i) = \mathbf{f}_n^{\mathcal{H}}\mathbf{y}(i) = H(\rho_n)s(iN+n) + w_n(i) \quad (3)$$

where $w_n(i) := \mathbf{f}_n^{\mathcal{H}}\bar{\mathbf{w}}(i)$ has variance σ_w^2.

C. Spread-Spectrum (SS)-OFDM and Multicarrier (MC)-CDMA

It is clear from (3) that if the channel $H(z)$ exhibits a deep fade at ρ_n, the transmitted symbol $s(iN+n)$ can not be recovered—a manifestation of the fact that uncoded OFDM loses multipath diversity. To robustify the performance against channel fades and enable multipath diversity, spread-spectrum (SS)-OFDM has been proposed in [7], [13] and [14]. SS-OFDM is essentially a repeated transmission, whereby different copies of each information symbol are transmitted over all available N subcarriers. With $\mathbf{c} = [c(0), \ldots, c(N-1)]^T$ denoting the spreading vector, the ith information-bearing block $\mathbf{s}(i)$ is formed by $\mathbf{s}(i) = \mathbf{c}s(i)$, and is transmitted using OFDM.

If $\mathbf{D}_h := \mathrm{diag}[H(\rho_0), \ldots, H(\rho_{N-1})]$, then collecting $r_n(i)$ in (3) into the vector $\mathbf{r}(i) = [r_0(i), \ldots, r_{N-1}(i)]^T$ (and likewise for $\mathbf{w}(i)$), we have

$$\mathbf{r}(i) = \mathbf{D}_h\mathbf{c}s(i) + \mathbf{w}(i). \quad (4)$$

On $\mathbf{r}(i)$, we perform maximum-ratio combining (MRC) to obtain the symbol estimate $\hat{s}(i) = \mathbf{c}^{\mathcal{H}}\mathbf{D}_h^{\mathcal{H}}\mathbf{r}(i)$. Upon selecting each entry of $\mathbf{c}$ to have constant modulus $1/\sqrt{N}$, we can express the signal-to-noise ratio (SNR) at the MRC output as

$$\|\mathbf{D}_h\mathbf{c}\|^2\frac{\sigma_s^2}{\sigma_w^2} = \sum_{n=0}^{N-1}\frac{1}{N}|H(\rho_n)|^2\frac{\sigma_s^2}{\sigma_w^2} = \mathbf{h}^{\mathcal{H}}\mathbf{h}\frac{\sigma_s^2}{\sigma_w^2} \quad (5)$$

where σ_s^2 is the symbol energy. Equation (5) testifies that SS-OFDM enables full multipath diversity that can be collected at the receiver by MRC.

SS-OFDM only transmits one information symbol per OFDM block, which comes at the price of considerable rate loss. To share the N subcarriers among multiple (say U) users, MC-CDMA has been advocated in [22], where different

users are distinguished by their signature codes $\{\mathbf{c}_u\}_{u=0}^{U-1}$. The received vector becomes

$$\mathbf{r}(i) = \sum_{u=0}^{U-1} \mathbf{D}_{h,u}\mathbf{c}_u s_u(i) + \mathbf{w}(i) \tag{6}$$

where $\mathbf{D}_{h,u}$ and $s_u(i)$ are the corresponding diagonal channel matrix and information symbol for user u. With $U \geq 2$, optimal decoding requires multiuser detection to cope with MUI. Besides requiring knowledge of all signature codes and user channels, the performance of MC-CDMA is upper bounded by SS-OFDM, because the latter corresponds to the best (interference-free) scenario, where all signals from other users have been correctly detected and subtracted. The performance of SS-OFDM can thus be viewed as the single-user performance bound on MC-CDMA.

D. OFDMA

To avoid MUI, OFDMA simply assigns to each user a distinct subcarrier from the set $\{\mathbf{f}_n\}_{n=0}^{N-1}$. If the assigned subcarrier to user u, denoted as $\bar{\mathbf{f}}_u(i)$, changes from block to block, one obtains a frequency-hopped (FH)-OFDMA system [12]. The ith transmitted chip block is thus $\mathbf{x}_u(i) = \bar{\mathbf{f}}_u(i)s_u(i)$, where $s_u(i)$ is the ith symbol of user u. The uth user's signals can then be expressed as

$$y_u(i) = \bar{\mathbf{f}}_u^{\mathcal{H}}(i)\mathbf{y}(i) = H_u\left(\rho_u^{(i)}\right)s_u(i) + \bar{\mathbf{f}}_u^{\mathcal{H}}(i)\bar{\mathbf{w}}(i) \tag{7}$$

where $\rho_u^{(i)}$ denotes the subcarrier assigned to the ith block of user u.

Let us now examine the properties of OFDMA transmissions. In uplink, each OFDMA user transmits one information symbol on one assigned subcarrier, which has constant modulus. Therefore, OFDMA is power efficient in the uplink. Taking into account the CP, and supposing full user load $(U = N)$, the bandwidth efficiency is defined as the maximum number of transmitted symbols per chip period T_c

$$\eta_1 = \frac{N}{N+L} \tag{8}$$

and approaches 100%, when $N \gg L$. But for systems with moderate N and large L, bandwidth efficiency may suffer. The block size N (or, the total number of subcarriers) needs to be enlarged in such cases, with each user using several subcarriers simultaneously.

As evidenced by (7), the performance of OFDMA degrades severely when the underlying channel undergoes deep fading around $\rho_u^{(i)}$. To cope with deep channel fades, incorporation of error-control coding (possibly in conjunction with FH) is imperative for OFDMA. The performance of coded OFDMA is discussed in Section IV.

E. GMC-CDMA

Linear precoding across OFDM subcarriers has been introduced as an alternative means of mitigating channel fades in GMC-CDMA systems [5], [17]. Instead of one subcarrier, $J > 1$ subcarriers $\{\bar{\mathbf{f}}_{u,j}\}_{j=0}^{J-1}$ are assigned to user u, to transmit $K > 1$ information symbols, simultaneously. Specifically, the ith information block

$$\mathbf{s}_u(i) := [s_u(iK+0), \ldots, s_u(iK+K-1)]^T$$

is precoded using a $J \times K$ tall $(J > K)$ precoder $\mathbf{\Theta}$ to obtain $\tilde{\mathbf{s}}_u(i) := \mathbf{\Theta}\mathbf{s}_u(i)$. The $J \times 1$ precoded blocks $\tilde{\mathbf{s}}_u(i)$ are then transmitted over the assigned J subcarriers. The redundancy offered by $\mathbf{\Theta}$ ensures that symbols can be recovered (perfectly in the absence of noise) regardless of the channel zero locations, provided that $J \geq K + L$ [5], [17]. In addition to symbol recovery, it has been established that linear precoding (a.k.a. complex field coding) enables the maximum multipath diversity [18].

Let us now check the power and bandwidth efficiency of GMC-CDMA. By using J subcarriers per user, GMC-CDMA does not possess constant modulus transmissions, in general.[1] For a maximum number of U users, $UJ = U(K+L)$ subcarriers are needed to carry UK information symbols. Taking into account the CP, the bandwidth efficiency is thus

$$\eta_2 = \frac{UK}{U(K+L)+L} \approx \frac{K}{K+L}. \tag{9}$$

To achieve high bandwidth efficiency, one should choose K as large as possible [5], [17]. However, in practice, the choice of K may be limited by other factors. For example, the channels are slowly time varying, thus posing an upper bound on the OFDM block duration $U(K+L)T_c$, during which the channels can be viewed as time invariant so that subcarrier orthogonality is preserved. As L increases, the spectral efficiency of GMC-CDMA becomes increasingly limited.

III. UP-OFDMA

In this section, we develop a UP-OFDMA scheme that achieves improved performance, yet with high bandwidth efficiency. Furthermore, we show that UP-OFDMA preserves constant modulus transmissions in the uplink, and is, therefore, power efficient as well.

A. Bandwidth- and Power-Efficient Transmissions

Distinct from *redundant* precoding utilized by GMC-CDMA [17], we propose here *nonredundant* unitary precoding across OFDMA subcarriers. Specifically, we allocate K subcarriers $\{\bar{\mathbf{f}}_{u,k}(i)\}_{k=0}^{K-1}$ per user to transmit K information symbols during the ith block interval. For comparison purposes, we will consider a system with the maximum number of users $U = N$. This multiuser system relies on $P = NK$ subcarriers, and requires an IFFT of size P. The total duration of each transmitted block is thus $(P+L)T_c = (NK+L)T_c$ after CP insertion.

The ith $K \times 1$ information block $\mathbf{s}_u(i)$ is precoded by a $K \times K$ square matrix $\mathbf{\Theta}$ to obtain $\tilde{\mathbf{s}}_u(i) = \mathbf{\Theta}\mathbf{s}_u(i)$, with its entries transmitted on K distinct subcarriers. Collecting the outputs $\bar{\mathbf{f}}_{u,k}^{\mathcal{H}}(i)\mathbf{y}(i)$ on those K subcarriers for user u into the

[1]Interestingly, as shown in [17], there is a way to allocate multiple subcarriers per user, and still ensure constant modulus transmissions.

vector $\mathbf{y}_u(i)$, we arrive at the equivalent block input–output relationship

$$\mathbf{y}_u(i) = \mathbf{\Lambda}_u(i)\mathbf{\Theta}\mathbf{s}_u(i) + \mathbf{w}_u(i) \tag{10}$$

where $\mathbf{\Lambda}_u(i) := \text{diag}\left[H_u\left(\rho_{u,0}^{(i)}\right), \ldots, H_u\left(\rho_{u,K-1}^{(i)}\right)\right]$ collects the channel frequency response samples during the ith block, and $\mathbf{w}_u(i)$ is the resulting AWGN with variance σ_w^2 per entry. The block index i on $\mathbf{\Lambda}_u(i)$ signifies the fact that we allow the channel frequency response to change from block to block due to channel variation and/or FH.

We look for a $\mathbf{\Theta}$ that optimizes error performance, while at the same time maintains constant modulus transmissions. To achieve both of these objectives, we will assign multiple subcarriers per user and choose the precoder $\mathbf{\Theta}$ judiciously. To this end, we first assign maximally (but equi-) spaced subcarriers to each user as follows:

$$\rho_{u,k}^{(i)} = e^{j2\pi(u+i+kN)/P}, \quad \forall\, k \in [0, K-1],\ u \in [0, N-1]. \tag{11}$$

The motivation behind (11) is to separate the subcarriers as much as possible, so that they are less correlated. From block to block, we take the indexes of the assigned subcarriers to increase by one, in the spirit of the one-step FH in [12]. Although alternate FH patterns can be implemented in practice, we stick to (11) for simplicity.

We will choose the UP matrix as in [4] and [21]

$$\mathbf{\Theta} = \mathbf{F}_K\bar{\mathbf{\Delta}} \tag{12}$$

where $\bar{\mathbf{\Delta}} := \text{diag}\{1, e^{-j\pi/(2K)}, \ldots, e^{-j(K-1)\pi/(2K)}\}$ is a diagonal matrix with unit-amplitude diagonal entries. Notice that our $\mathbf{\Theta}$ in (12) is the conjugated version of the precoders used in [19] and [21] (conjugation does not affect the performance). We will prove the following.

Proposition 1: The equispaced subcarrier assignment (11), together with the precoder (12), leads to perfectly constant modulus UP-OFDMA user transmissions.

Proof: Suppose that the symbols in $\mathbf{s}_u(i)$ are drawn from a phase-shift keying (PSK) constellation. The transmitted signal can be written as

$$\mathbf{x}_u(i) = \mathbf{F}_P^{\mathcal{H}}\mathbf{\Psi}_u(i)\mathbf{\Theta}\mathbf{s}_u(i)$$

where $\mathbf{\Psi}_u(i)$ is the $P \times K$ subcarrier selection matrix, with the K columns being the K unit vectors whose nonzero entries are positioned according to the subcarriers assigned to user u. With the subcarrier assignment (11), the kth subcarrier for user u is the $[(u+i+kN)+1]$st column of the IFFT matrix $\mathbf{F}_P^{\mathcal{H}}$. We thus verify that the $(p+1, k+1)$st entry of $\mathbf{F}_P^{\mathcal{H}}\mathbf{\Psi}_u(i)$ is

$$\left[\mathbf{F}_P^{\mathcal{H}}\mathbf{\Psi}_u(i)\right]_{p,k} = \frac{1}{\sqrt{N}}e^{[j2\pi p(u+i)/P]}\frac{1}{\sqrt{K}}e^{j2\pi pk/K}. \tag{13}$$

For notational brevity, let us define two constants $\omega_0 := \exp(j2\pi/P)$, and $\alpha := 1/\sqrt{N}$. With M signifying dimensionality, we construct the $M \times 1$ vector $\mathbf{v}_M(\omega) := [1, \omega, \ldots, \omega^{M-1}]^T$, and the $M \times M$ diagonal matrix $\mathbf{\Delta}_M(\omega) := \text{diag}[\mathbf{v}_M(\omega)]$ from a scalar ω. It follows from (13) that $\mathbf{F}_P^{\mathcal{H}}\mathbf{\Psi}_u(i) = \alpha\mathbf{\Delta}_P\left(\omega_0^{u+i}\right)\left(\mathbf{1}_{N\times 1} \otimes \mathbf{F}_K^{\mathcal{H}}\right)$. We first verify that

$$\mathbf{\Delta}_P\left(\omega_0^{u+i}\right) = \mathbf{\Delta}_P\left(\omega_0^{i}\right)\mathbf{\Delta}_P\left(\omega_0^{u}\right)$$

and

$$\mathbf{\Delta}_P\left(\omega_0^{u}\right) = \mathbf{\Delta}_N\left(\omega_0^{Ku}\right) \otimes \mathbf{\Delta}_K(\omega_0).$$

Using the property of Kronecker products

$$(\mathbf{A}_1 \otimes \mathbf{A}_2)(\mathbf{A}_3 \otimes \mathbf{A}_4) = (\mathbf{A}_1\mathbf{A}_3) \otimes (\mathbf{A}_2\mathbf{A}_4)$$

we obtain

$$\mathbf{F}_P^{\mathcal{H}}\mathbf{\Psi}_u(i) = \alpha\mathbf{\Delta}_P\left(\omega_0^{i}\right)\left[\mathbf{v}_N\left(\omega_0^{Ku}\right) \otimes \left(\mathbf{\Delta}_K(\omega_0)\mathbf{F}_K^{\mathcal{H}}\right)\right]. \tag{14}$$

Consequently, we simplify the transmitted block as

$$\begin{aligned}\mathbf{x}_u(i) &= \mathbf{F}_P^{\mathcal{H}}\mathbf{\Psi}_u(i)\mathbf{\Theta}\mathbf{s}(i) \\ &= \alpha\mathbf{\Delta}_P\left(\omega_0^{i}\right)\left[\mathbf{v}_N\left(\omega_0^{Ku}\right) \otimes \left(\mathbf{\Delta}_K(\omega_0)\bar{\mathbf{\Delta}}\right)\right]\mathbf{s}(i).\end{aligned} \tag{15}$$

It is clear from (15) that the transmitted sequence $\mathbf{x}_u(i)$ has constant modulus if the original sequence $\mathbf{s}_u(i)$ does; e.g., when $\mathbf{s}_u(i)$ is drawn from PSK constellations. Specifically, for $p = nK + k$, where $n = 0, \ldots, N-1$ and $k = 0, \ldots, K-1$, the $(p+1)$st entry of $\mathbf{x}_u(i)$ is

$$[\mathbf{x}_u(i)]_p = \alpha e^{j[2\pi p(u+i)/P]}e^{-jk\pi/(2K)}[\mathbf{s}_u(i)]_k. \tag{16}$$

■

Next, let us evaluate the bandwidth efficiency of UP-OFDMA and compare it with other systems. With each user transmitting K symbols over $P+L$ chips, the maximum bandwidth efficiency of UP-OFDMA is

$$\eta_3 = \frac{NK}{P+L} = \frac{N}{\frac{N+L}{K}} \approx 1. \tag{17}$$

Comparing (17) with (9), we see that the bandwidth efficiency of UP-OFDMA is larger than that of GMC-CDMA, in general. However, when comparing UP-OFDMA with conventional OFDMA, one has to distinguish between two cases.

1) If both systems are to accommodate the maximum number of users $U = N$, it follows from (17) and (8) that UP-OFDMA offers a K-fold decrease in the effective channel order, and achieves higher bandwidth efficiency than the conventional OFDMA. However, UP-OFDMA has increased the number of subcarriers from N to NK, which for the same bandwidth leads to reduced subcarrier spacing, and a longer OFDM symbol duration.
2) If both systems have the same OFDM symbol duration, and identical number of subcarriers, then they entail different parameters N, which we denote, respectively, as $N_{\text{UP-OFDMA}}$ and N_{OFDMA}. In this case, we have

$$K \cdot N_{\text{UP-OFDMA}} = N_{\text{OFDMA}}. \tag{18}$$

Plugging (18) into (17), we verify that UP-OFDMA has bandwidth efficiency identical to conventional OFDMA. In this case, the conventional OFDMA can either accommodate K times more users than UP-OFDMA, or assign multiple (K) subcarriers per user if the maximum number of users is kept the same. Unfortunately, by allocating multiple subcarriers per user, OFDMA will no longer have constant-modulus transmissions.

Summarizing, we have established the following.

Proposition 2: In general, UP-OFDMA enjoys higher bandwidth efficiency than GMC-CDMA. When both systems accommodate the same (maximum) number of users, UP-OFDMA has higher bandwidth efficiency than OFDMA,

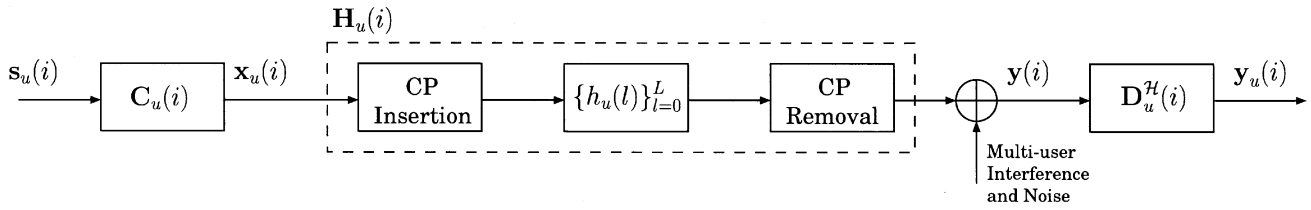

Fig. 1. System model based on block spreading and despreading.

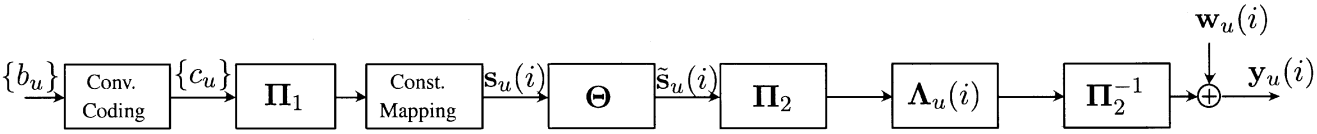

Fig. 2. Equivalent system model for coded UP-OFDMA.

while both systems have identical bandwidth efficiency when the total number of subcarriers is fixed.

B. A Block-Spreading (Multicode) Interpretation

A unifying framework based on block spreading and despreading has been developed in [17] that includes many existing CDMA schemes as special cases. In Section III-A, we have introduced UP-OFDMA from a multicarrier point of view. We now interpret it from a block-spreading perspective. As depicted in Fig. 1, the $K \times 1$ symbol block $\mathbf{s}_u(i)$ of user u is block spread by a $P \times K$ spreading matrix $\mathbf{C}_u(i)$, and then transmitted after CP insertion. At the receiver, CP is removed, and multiuser separation is performed through block despreading by the $K \times P$ matrix $\mathbf{D}_u(i)$. CP insertion at the transmitter, together with CP removal at the receiver, result in the following block input–output relationship [17]:

$$\mathbf{y}(i) = \sum_{u=0}^{U-1} \mathbf{H}_u(i)\mathbf{C}_u(i)\mathbf{s}_u(i) + \bar{\mathbf{w}}(i) \tag{19}$$

where $\mathbf{H}_u$ is a $P \times P$ circulant matrix with

$$[\mathbf{H}_u]_{i,j} = h_u((i-j) \bmod P).$$

The output of block despreading for the desired user μ is obtained as

$$\begin{aligned}\mathbf{y}_\mu(i) &:= \mathbf{D}_\mu^{\mathcal{H}}(i)\mathbf{y}(i) \\ &= \sum_{u=0}^{U-1} \mathbf{D}_\mu^{\mathcal{H}}(i)\mathbf{H}_u(i)\mathbf{C}_u(i)\mathbf{s}_u(i) + \mathbf{D}_\mu^{\mathcal{H}}(i)\bar{\mathbf{w}}(i). \end{aligned} \tag{20}$$

Relying on the general model of (19) and (20), the goal is to design the block-spreading matrices $\{\mathbf{C}_u(i)\}_{u=0}^{U-1}$ and the block-despreading matrices $\{\mathbf{D}_u(i)\}_{u=0}^{U-1}$. The objective is to guarantee deterministic multiuser separation without knowing the channels, so that one can simplify (20) to

$$\mathbf{y}_\mu(i) = \mathbf{D}_\mu^{\mathcal{H}}(i)\mathbf{H}_\mu(i)\mathbf{C}_\mu(i)\mathbf{s}_\mu(i) + \mathbf{D}_\mu^{\mathcal{H}}(i)\bar{\mathbf{w}}(i). \tag{21}$$

One such design example is provided in [23]. Our proposed UP-OFDMA in Section III-A fits into this general transceiver model as another example. Specifically, our (de)spreading matrices are

$$\begin{aligned}\mathbf{C}_u(i) &:= \alpha\mathbf{\Delta}_P\left(\omega_0^i\right)\left[\mathbf{v}_N\left(\omega_0^{Ku}\right) \otimes \left(\mathbf{\Delta}_K(\omega_0)\bar{\mathbf{\Delta}}\right)\right] \\ \mathbf{D}_u(i) &:= \alpha\mathbf{\Delta}_P\left(\omega_0^i\right)\left[\mathbf{v}_N\left(\omega_0^{Ku}\right) \otimes \left(\mathbf{\Delta}_K(\omega_0)\mathbf{F}_K^{\mathcal{H}}\right)\right]. \end{aligned} \tag{22}$$

The diagonal matrix $\mathbf{\Delta}_P(\omega_0^i)$ in $\mathbf{C}_u(i)$ can be viewed as a long scrambling code that changes from block to block.

It can be readily checked that our design of spreading and despreading matrices in (22) ensures mutual orthogonality among users, i.e., $\mathbf{C}_u^{\mathcal{H}}(i)\mathbf{C}_{u'}(i) = \mathbf{I}_K\delta(u-u')$ and $\mathbf{D}_u^{\mathcal{H}}(i)\mathbf{D}_{u'}(i) = \mathbf{I}_K\delta(u-u')$. Plugging (22) into (20), one can end up with (10).

IV. Performance of Coded UP-OFDMA

So far, we have considered an uncoded UP-OFDMA system, that is both power and bandwidth efficient. In this section, we demonstrate that unitary precoding also improves error performance considerably. Since error-control coding is always employed in practical systems, we will analyze a convolutionally encoded UP-OFDMA system. The equivalent system model with convolutional coding (CC) is depicted in Fig. 2. Specifically, the binary information bits are encoded by the convolutional encoder and interleaved by the bit interleaver $\mathbf{\Pi}_1$. After constellation mapping and unitary precoding, the precoded symbols go through a symbol interleaver $\mathbf{\Pi}_2$, and propagate over parallel flat-fading subchannels that are assigned to each user. The interleaver $\mathbf{\Pi}_2$ is introduced to interleave the channel's frequency response across UP-OFDMA blocks. With sufficiently large $\mathbf{\Pi}_2$ and relatively fast channel variation, the interleaved channel response can be viewed as (at least approximately) uncorrelated. On the other hand, when the interleaver size is not large enough, channel correlation should be taken into account.

We will analyze the performance of coded UP-OFDMA, to reveal the benefit induced by unitary precoding, and also to quantify the power savings over conventional OFDMA in a simplified fading channel. We consider maximum-likelihood (ML) optimal decoding at the receiver to carry out the theoretical analysis. In practice, effective iterative (turbo) decoders can be employed, including those derived in [6], [16], and [19]. Compared to conventional OFDMA, the iterative receiver improves the performance of UP-OFDMA at the price of increased complexity. However, for small or moderate values of the block size K, the receiver complexity is quite affordable [6], [16], [19]. A related performance analysis has also been carried out in [19] for single-user OFDM systems in the presence of Rayleigh fading channels. Our analysis here extends the results of [19] to UP-OFDMA and Ricean fading.

Since signals from multiple users are separated at the receiver, we will, henceforth, focus on a single user only, and drop the user index u for notational brevity. Let $\underline{\mathbf{c}} := (c(0), c(1), c(2), \ldots)$ denote one realization of the coded bit sequence, $\underline{\mathbf{s}} := (s(0), s(1), s(2), \ldots)$ the corresponding symbol sequence after the interleaver $\mathbf{\Pi}_1$ and the constellation mapper, and $\underline{\mathbf{y}} := (y(0), y(1), y(2), \ldots)$ the received sequence after deinterleaving by $\mathbf{\Pi}_2^{-1}$. Similarly, let $\underline{\hat{\mathbf{c}}}$, $\underline{\hat{\mathbf{s}}}$, and $\underline{\hat{\mathbf{y}}}$ be the corresponding quantities for another realization.

Assume that $\underline{\mathbf{c}}$ and $\underline{\hat{\mathbf{c}}}$ differ in d bits. With the interleaver $\mathbf{\Pi}_1$ designed properly, these d bits are scrambled such that no two bits fall into the same symbol block. This assumption is based on the fact that the block size K is small in practice, and its validity will be corroborated by simulation results. Suppose that after interleaving, those d different symbols, labeled as $s(n_1), s(n_2), \ldots, s(n_d)$, fall into blocks $\mathbf{s}(b_1), \mathbf{s}(b_2), \ldots, \mathbf{s}(b_d)$, with $m_1, m_2, \ldots, m_d$ describing the positions of these symbols in their corresponding blocks. In other words, we have $n_w = b_w K + m_w$ and $s(n_w) = [\mathbf{s}(b_w)]_{m_w}$, $\forall w \in [1, d]$. Define the precoded block as $\tilde{\mathbf{s}}(b_w) = \mathbf{\Theta}\mathbf{s}(b_w)$, and let $\boldsymbol{\theta}_k^T$ denote the kth row of $\mathbf{\Theta}$. The $(k+1)$st entry of $\tilde{\mathbf{s}}(b_w)$ is thus $[\tilde{\mathbf{s}}(b_w)]_k = \boldsymbol{\theta}_k^T \mathbf{s}(b_w)$.

Dropping the user index in (10), and letting $\lambda(b_w K + k)$ denote the $(k+1, k+1)$st entry of the diagonal matrix $\mathbf{\Lambda}(b_w)$, we obtain the serial version of (10) as

$$y(b_w K + k) = \lambda(b_w K + k)\boldsymbol{\theta}_k^T \mathbf{s}(b_w) + w(b_w K + k) \quad (23)$$

where $k \in [0, K-1]$, and $w \in [1, d]$. Similarly, we have $\hat{y}(b_w K + k)$ corresponding to $\underline{\hat{\mathbf{s}}}$.

Define

$$\bar{\mathbf{s}}(b_w) := \mathbf{s}(b_w) - \hat{\mathbf{s}}(b_w)$$
$$\bar{y}(b_w K + k) := y(b_w K + k) - \hat{y}(b_w K + k).$$

Notice that only one symbol discrepancy occurs in each of the d inconsistent blocks. Therefore

$$\bar{\mathbf{s}}(b_w) = [0, \ldots, 0, \bar{s}(n_w), 0, \ldots, 0]^T$$

and $\boldsymbol{\theta}_k^T \bar{\mathbf{s}}(b_w) = \theta_{k,m_w} \bar{s}(n_w)$, where θ_{k,m_w} is the $(k+1, m_w+1)$st entry of $\mathbf{\Theta}$. We then obtain

$$\bar{y}(b_w K + k) = \lambda(b_w K + k)\theta_{k,m_w} \bar{s}(n_w). \quad (24)$$

Each single error $\bar{s}(n_w)$ will lead to K different received symbols through K subcarriers. This intuitively explains why precoding enables full multipath diversity.

Other than the differences introduced by $\{\bar{s}(n_w)\}_{w=1}^d$, the received sequences $\underline{\mathbf{y}}$ and $\underline{\hat{\mathbf{y}}}$ are the same. The Euclidean distance between $\underline{\mathbf{y}}$ and $\underline{\hat{\mathbf{y}}}$ can be found as

$$D^2(\underline{\mathbf{y}}, \underline{\hat{\mathbf{y}}}) = \sum_{w=1}^{d} \sum_{k=0}^{K-1} |\lambda(b_w K + k)\theta_{k,m_w} \bar{s}(n_w)|^2 \geq \frac{\delta^2}{K} \sum_{w=1}^{d} \sum_{k=0}^{K-1} |\lambda(b_w K + k)|^2 \quad (25)$$

where δ is the minimum distance between any two symbols in the adopted signal constellation. The derivation of (25) takes into account that each entry of $\mathbf{\Theta}$ has amplitude $1/\sqrt{K}$. Thus, for each channel realization, the conditional pairwise error probability that $\underline{\hat{\mathbf{c}}}$ is decided when $\underline{\mathbf{c}}$ is actually transmitted, can be upper bounded as

$$P_E\{\underline{\mathbf{c}} \to \underline{\hat{\mathbf{c}}} \mid \text{channel}\} = \mathcal{Q}\left(\sqrt{\frac{D^2(\underline{\mathbf{y}}, \underline{\hat{\mathbf{y}}})}{2N_0}}\right) \leq \mathcal{Q}\left(\sqrt{\frac{\delta^2 \left(\sum_{w=1}^{d} \sum_{k=0}^{K-1} |\lambda(b_w K + k)|^2\right)}{2KN_0}}\right). \quad (26)$$

This conditional pairwise error probability needs to be averaged over all channel realizations. Therefore, we need to find the probability distribution of each channel value $\lambda(b_w K + k)$, as well as the correlations of those channel values across different blocks and subcarriers.

Rayleigh fading on each FIR channel tap is usually assumed for simplicity. Ricean fading, however, is more general, in that it includes Rayleigh fading as a special case when no line-of-sight (LOS) is present [11]. Specifically, we will assume that the first nonzero channel tap (corresponding to the LOS signal) for each user is modeled as Ricean faded, while the remaining channel taps are Rayleigh faded and uncorrelated. The channel's frequency response values $\lambda(b_w K + k)$ will be Ricean faded with the same Ricean factors $\mathcal{K}$ across different subcarriers. In practice, due to the transmit–receive filters and chip-rate sampling, more than one channel tap may be Ricean faded even when only one physical LOS path is present. In such a case, $\lambda(b_w K + k)$ will be Ricean faded with carrier-specific Ricean factors. For illustration purposes, we will adopt the simple Ricean fading channel model, assuming that the frequency response values on the K subcarriers of each user are independently and identically Ricean faded.

Since the coded bit sequence will be transmitted over multiple blocks, we also need to consider the channel frequency response across different blocks. In mobile communication systems, the channels are slowly varying due to the terminal mobility, or the changing scattering environment. Interleaving, via $\mathbf{\Pi}_2$, offers an effective means of improving performance in slowly fading channels. However, the interleaving depth is usually limited in many delay-sensitive applications, such as voice and certain data communication systems. In the following, we consider two extreme cases: first, *uncorrelated fading channels* with channel frequency responses uncorrelated from block to block, assuming that the interleaving depth is sufficiently large and the channels vary relatively fast; and second, *block fading channels* that are time invariant from block to block, assuming a static channel and no interleaving. These two models are rather idealistic, and practical systems employing limited interleaving will demonstrate a performance in between these extreme cases. However, through the study of these two extreme cases, we will illustrate the benefit of unitary precoding, and quantify the power savings of UP-OFDMA relative to conventional OFDMA, as well as the performance gap between UP-OFDMA and the single-user bound. This analysis provides theoretical insights and, more importantly, it offers practical guidelines for choosing the block size K.

A. Uncorrelated Fading Channels

Frequency responses on the subcarriers are Ricean distributed with Ricean factor $\mathcal{K}$, and they are uncorrelated from subcarrier to subcarrier, and from block to block. When $\mathcal{K}=0$, this channel model boils down to Rayleigh fading. Using the Chernoff bound $\mathcal{Q}(x) \leq 0.5\exp(-x^2/2)$, and averaging over random channels [10], [15], we arrive at the average pairwise error probability

$$P_E(d) := P_E\{\underline{\mathbf{c}} \to \hat{\underline{\mathbf{c}}}\} \leq \frac{1}{2}\left(\frac{1+\mathcal{K}}{\gamma_1}\cdot e^{-\mathcal{K}(1-(\mathcal{K}+1)/\gamma_1)}\right)^{Kd} \tag{27}$$

where $\gamma_1 := 1+\mathcal{K}+\delta^2/(4KN_0)$. The union bound on the bit-error rate (BER) can then be obtained as

$$\begin{aligned} P_b &\leq \sum_{d=d_f}^{\infty} B_d \mathrm{P}_E(d) \\ &= \frac{1}{2}\sum_{d=d_f}^{\infty} B_d \left(\frac{1+\mathcal{K}}{\gamma_1}\cdot e^{-\mathcal{K}(1-(\mathcal{K}+1)/\gamma_1)}\right)^{Kd} \end{aligned} \tag{28}$$

where the (B_d, d) pair is the bit distance spectrum of the CC [3]. At sufficiently high SNR, $P_b \sim (\gamma_1)^{-Kd_f}$ indicates that the diversity order of our UP-OFDMA is Kd_f, which amounts to a multiplicative diversity-order enhancement, due to precoding at the transmitter. The special case with $K=1$ reduces to conventional OFDMA with CC.

For $K \geq 2$, we define the SNR gain G_K as the reduction in SNR that is afforded by UP-OFDMA to achieve the same error performance as the conventional OFDMA. Targeting this prescribed performance, let δ_1 and δ_K be the minimum constellation distance needed for OFDMA and UP-OFDMA, respectively. The SNR gain G_K can be obtained by equating the average performance in (28) for both systems. As nonlinear equations must be solved to obtain G_K, no closed form is possible. However, this could be circumvented by approximating the Ricean-$\mathcal{K}$ distribution using the Nakagami-m distribution, with the two factors related as $m=(1+\mathcal{K})^2/(1+2\mathcal{K})$ [15, p. 23], where $\mathcal{K}\geq 0$ and $m \geq 1$. Recall that Rayleigh fading corresponds to $m=1$. Hence, in a similar way, we average the pairwise error probability again using the Nakagami distribution, which yields

$$\mathrm{P}_E(d) \leq \frac{1}{2}\left(1+\frac{\delta^2}{4mKN_0}\right)^{-mKd}. \tag{29}$$

And similarly, the BER is upper bounded by

$$\mathrm{P}_b \leq \frac{1}{2}\sum_{d=d_f}^{\infty} B_d \left(1+\frac{\delta^2}{4mKN_0}\right)^{-mKd}. \tag{30}$$

We verify that these two bounds in (28) and (30) are almost identical for the error rates considered (below 10^{-6}). Therefore, approximating the Ricean distribution using the Nakagami-m distribution is well justified, and allows us to find G_K in closed form.

Plugging δ_1 and δ_K into (30) for OFDMA and UP-OFDMA, the SNR gain G_K to achieve the same performance can be readily obtained as

$$G_K = \frac{\delta_1^2}{\delta_K^2} = \frac{\delta_1^2}{4mKN_0\left[\left(1+\frac{\delta_1^2}{4mN_0}\right)^{1/K}-1\right]}. \tag{31}$$

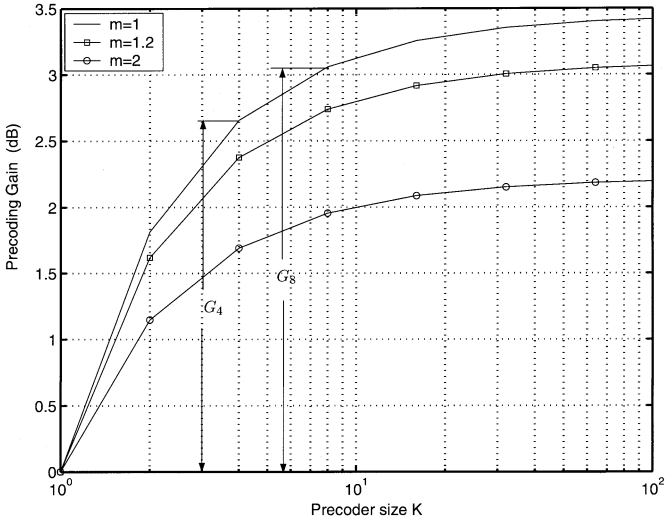

Fig. 3. SNR gain of UP-OFDMA over OFDMA.

We now quantify the performance gap of UP-OFDMA with respect to the single-user bound. We assume a rich scattering environment, where the $L+1$ channel taps are uncorrelated. As stated in [24], the performance of SS-OFDM can be achieved with only $L+1$ equispaced subcarriers. Therefore, the single-user bound as described in Section II-C can be quantified by setting $K=L+1$ in (28) and (30). Following that, we define the SNR gap between our UP-OFDMA and the single-user bound as

$$\epsilon_K := \frac{\delta_K^2}{\delta_{L+1}^2} = \frac{K\left[\left(1+\frac{\delta_1^2}{4mN_0}\right)^{1/K}-1\right]}{(L+1)\left[\left(1+\frac{\delta_1^2}{4mN_0}\right)^{1/(L+1)}-1\right]}. \tag{32}$$

Fig. 3 depicts the SNR gain G_K for different block sizes K and typical values of the Nakagami factor m (or the Ricean factor $\mathcal{K}$), where we set $\delta_1^2/N_0 = 11$ dB, which amounts to $E_b/N_0 = 6.7$ dB for a rate 2/3 code and binary PSK modulation. It is evident that G_K saturates quickly as K increases. Most performance improvement is observed for $K \leq 10$. The SNR gain of the single-user SS-OFDM over conventional OFDMA can be found in Fig. 3 by setting $K = L+1$. For all the different m's, the additional performance improvement by increasing $K=4$ to $K=L+1$ (the single-user bound) is less than 1 dB, even for very large L. For sparse channels with small $\tilde{L}_u$, the performance gap decreases further, since those $L+1$ taps become highly correlated. We therefore conclude that our UP-OFDMA (with $K \geq 4$) is very effective, with each user having performance close to the single-user bound. Also, notice that the single-user bound, as well as the SNR gap ϵ_K, decreases as m increases; i.e., when the channel condition improves.

From a BER perspective, K should be chosen as large as possible. However, in practice, the choice of K is limited by many factors. First, the channel must be ensured time invariant during each block of duration $(NK+L)T_c$. Increasing K unrestrictedly can render this assumption no longer valid. Second, the decoding complexity increases when K increases. Furthermore, for sparse channels with small $\tilde{L}_u$, the K subcarriers of each user will be highly correlated if $K > \tilde{L}_u$. All these motivate

and well justify choosing a small K for UP-OFDMA. In practice, K can be chosen to be smaller than 12, e.g., $K = 4, 8$. The performance gap from the single-user bound is less than 1 dB in the presence of ideal uncorrelated fading channels.

B. Block Fading Channels

In block fading channels, we assume that the link remains time invariant across blocks. And we also assume that interleaving and/or FH are not used, so that multipath diversity is not fully enabled by UP-OFDMA. For such a setup, the pairwise error probability can be similarly bounded as

$$P_E(d) := P_E\{\underline{\mathbf{c}} \to \hat{\underline{\mathbf{c}}}\} \le \frac{1}{2}\left(\frac{1+\mathcal{K}}{\gamma_2}\cdot e^{-\mathcal{K}(1-(\mathcal{K}+1)/\gamma_2)}\right)^K \quad (33)$$

where $\gamma_2 := 1 + \mathcal{K} + d\cdot\delta^2/(4KN_0)$. The union bound on the BER can then be obtained as

$$P_b \le \sum_{d=d_f}^{\infty} B_d P_E(d) = \frac{1}{2}\sum_{d=d_f}^{\infty} B_d\left(\frac{1+\mathcal{K}}{\gamma_2}\cdot e^{-\mathcal{K}(1-(\mathcal{K}+1)/\gamma_2)}\right)^K. \quad (34)$$

We see that the diversity order is K here, much less than Kd_f in the uncorrelated fading scenario. In such cases, CC only contributes to the coding gain rather than the diversity gain. The performance of such systems will suffer from limited diversity. For example, when $K = 1$, the diversity of conventional OFDMA is only one. When the channel has a deep null on the assigned subcarrier, the transmitted signals can not be recovered. This highly motivates FH to benefit from multipath diversity, and coding together with interleaving to enable time diversity. Antenna (or space) diversity is another form of diversity that can be incorporated easily in our UP-OFDMA system, following the approach in [9]. Since for this case, it is difficult to obtain the SNR gain G_K in closed form, simulations will be used to verify the performance improvement.

V. Simulations

We present numerical results in this section. We assume $P = 64$ subcarriers in the system and allocate $K = 4$ subcarriers per user. We use the rate 2/3 CC with generator polynomial $[3\ 1\ 0; 2\ 3\ 3]$, and bit distance spectrum polynomial $B(z) = 0.5z^3 + 3z^4 + 8z^5 + 23z^6 + \cdots$ [3]. We use binary PSK modulation and let each frame contain 192 information bits. A block interleaver $\mathbf{\Pi}_1$ of dimension 18×16 is employed. At the receiver, we adopt the turbo decoding algorithm of [19]. For all simulations, the BER after three iterations will be plotted.

A. Uncorrelated Fading Channel

First, we simulate a rich scattering environment, with the channels independently Rayleigh faded from block to block (an idealized fast fading scenario that can be approximated through sufficiently long interleaving together with FH). Fig. 4 depicts the simulated BER of UP-OFDMA with $K = 4$, compared against conventional OFDMA with $K = 1$. Performance of single-user SS-OFDM is plotted with an underlying FIR channel of length eight. For reference, the union bounds in (28) are also plotted. First, we observe that the simulated BERs lie within 1 dB of the corresponding union bounds, which clearly validates our analytical result. When K increases from one to four, UP-OFDMA outperforms the conventional OFDMA considerably. At the same time, UP-OFDMA is less than 1 dB away from the single-user SS-OFDM, which is the lower bound achievable in the presence of multipath fading.

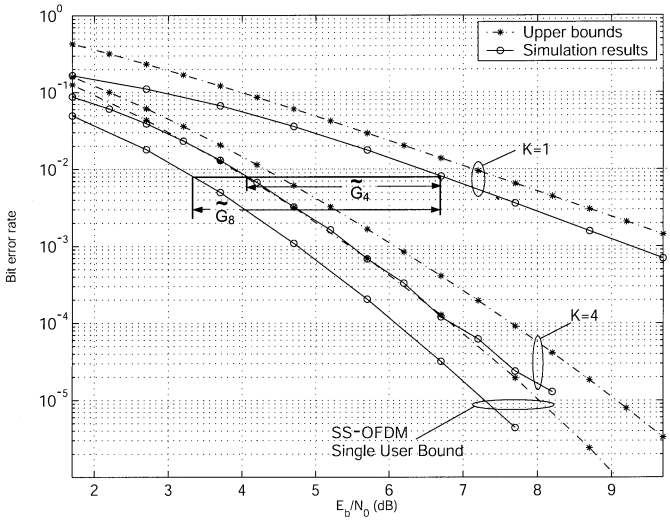

Fig. 4. Simulated performance of UP-OFDMA: uncorrelated fading channels.

In Fig. 3, we predicted the SNR gain G_K analytically through (31). Alternatively, we can also estimate those SNR gains through Monte–Carlo simulations. Actually, the estimates can be read directly from Fig. 4. For example, when $E_b/N_0 = 6.7$ dB and $m = 1$, the closed-form expression (30) predicts $G_4 = 2.6$ dB and $G_8 = 3.0$ dB, while Monte–Carlo simulations estimate $\tilde{G}_4 = 2.6$ dB, and $\tilde{G}_8 = 3.3$ dB. The fact that analytical and simulation-based results are very close demonstrates that the approximation in (31) is indeed sufficiently accurate.

B. Block-Fading Channel

We now consider a block-fading channel with 14 independent taps, and channels assumed to be constant per frame. BER curves of UP-OFDMA, as plotted in Fig. 5, fall within 0.5 dB of the union bound. For conventional OFDMA, the union bound becomes quite loose. Again, substantial performance improvement is observed, due to unitary precoding. Compared with the perfect interleaving case in Fig. 4, the performance suffers due to lack of time diversity. To fully exploit multipath diversity, FH is also simulated here with the hopping pattern selected according to (11). Again, UP-OFDMA improves performance over conventional OFDMA considerably.

C. Correlated Fading Channel

We have verified our analysis for the two extreme cases. Here, we investigate practical slow fading channels with $\mathbf{\Pi}_2$ having limited depth. We consider a correlated fading channel with $L+1 = 8$ equipowered channel taps. The carrier frequency is 5 GHz and the mobile velocity is 3 m/s, which results in a Doppler frequency of $f_m = 50$ Hz. The channel coherence time can be

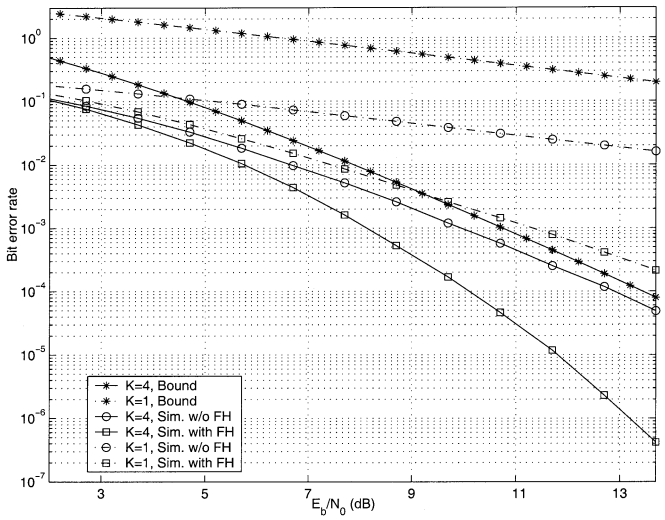

Fig. 5. Simulated performance of UP-OFDMA: block-fading channels.

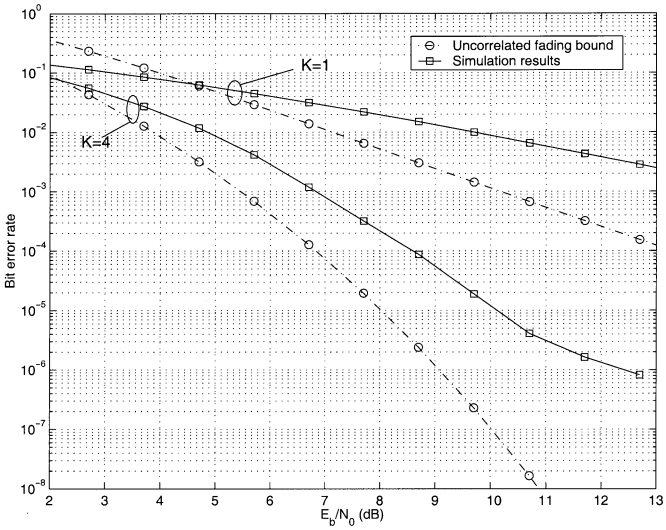

Fig. 6. Simulated performance of UP-OFDMA under correlated fading channels with limited interleaving.

computed as $\tau_c \approx 0.423/f_m = 8.5$ ms, using the empirical formula in [11, p. 166]. The chip rate in the simulation is taken as 1.152 MHz with chip duration $T_c = 0.87$ μs. For $\mathbf{\Pi}_2$, we study a block interleaver of size 144×128, inducing a delay of 16 ms $\approx 2\tau_c$. Under this practical channel, UP-OFDMA achieves an SNR improvement of about 7 dB, even for a high BER of 3×10^{-3}. Fig. 6 also illustrates that correlated fading incurs considerable performance loss relative to the ideal scenario with uncorrelated fading channels.

VI. Conclusions

In this paper, we developed a UP-OFDMA scheme, that is both bandwidth and power efficient for uplink applications. Performance analysis and simulation results revealed that UP-OFDMA improves performance considerably over existing alternatives.[2]

[2]The views and conclusions contained in this document are those of the authors and should not be interpreted as representing the official policies, either expressed or implied, of the Army Research Laboratory or the U. S. Government.

References

[1] (1999) 3GPP-TSG-RAN-WG4; UTRA (BS) TDD; Radio Transmission and Reception. Eur. Telecommun. Standards Inst. (ETSI), Sophia Antipolis, France. [Online]. Available: http://www.etsi.org/umts

[2] "Broadband Radio Access Networks (BRAN), Inventory of Broadband Radio Technologies and Techniques," Eur. Telecommun. Standards Inst. (ETSI), Sophia Antipolis, France, ref. DTR/BRAN 030 001, 1998.

[3] S. Benedetto and E. Biglieri, *Principles of Digital Transmission With Wireless Applications*. New York: Kluwer/Plenum, 1999.

[4] J. Boutros and E. Viterbo, "Signal space diversity: A power and bandwidth efficient diversity technique for the Rayleigh fading channel," *IEEE Trans. Inform. Theory*, vol. 44, pp. 1453–1467, July 1998.

[5] G. B. Giannakis, Z. Wang, A. Scaglione, and S. Barbarossa, "AMOUR-generalized multicarrier transceivers for blind CDMA regardless of multipath," *IEEE Trans. Commun.*, vol. 48, pp. 2064–2076, Dec. 2000.

[6] B. M. Hochwald and S. ten Brink, "Achieving near-capacity on a multiple-antenna channel," *IEEE Trans. Commun.*, vol. 51, pp. 389–399, Mar. 2003.

[7] S. Kaiser and K. Fazel, "A flexible spread spectrum multicarrier multiple-access system for multimedia applications," in *Proc. 8th IEEE Int. Symp. PIMRC*, vol. 1, 1997, pp. 100–104.

[8] I. Koffman and V. Roman, "Broadband wireless access solutions based on OFDM access in IEEE802.16," *IEEE Commun. Mag.*, pp. 96–103, Apr. 2002.

[9] Z. Liu and G. B. Giannakis, "Space–time block-coded multiple access through frequency-selective fading channels," *IEEE Trans. Commun.*, vol. 49, pp. 1033–1044, June 2001.

[10] J. G. Proakis, *Digital Communications*, 4th ed. New York: McGraw-Hill, 2000.

[11] T. Rappaport, *Wireless Communications: Principle and Practice*. Englewood Cliffs, NJ: Prentice-Hall, 1996.

[12] H. Sari and G. Karam, "Orthogonal frequency-division multiple access and its application to CATV network," *Eur. Trans. Telecommun.*, vol. 9, pp. 507–516, Nov./Dec. 1998.

[13] G. J. Saulnier, M. Mettke, and M. J. Medley, "Performance of an OFDM spread-spectrum communication system using lapped transforms," in *Proc. MILCOM Conf.*, 1997, pp. 608–612.

[14] G. J. Saulnier, Z. Ye, and M. J. Medley, "Performance of a spread-spectrum OFDM system in a dispersive fading channel with interference," in *Proc. MILCOM Conf.*, 1998, pp. 679–683.

[15] M. K. Simon and M.-S. Alouini, *Digital Communications Over Fading Channels: A Unified Approach to Performance Analysis*. New York: Wiley, 2000.

[16] B. Steingrimsson, Z. Luo, and K. M. Wong, "Soft quasi-maximum-likelihood detection for multiple-antenna channels," in *Proc. Int. Conf. Communications*, vol. 4, Anchorage, AK, May 11–15, 2003, pp. 2330–2334.

[17] Z. Wang and G. B. Giannakis, "Wireless multicarrier communications: Where Fourier meets Shannon," in *IEEE Signal Processing Mag.*, vol. 17, May 2000, pp. 29–48.

[18] ——, "Complex-field coding for OFDM over fading wireless channels," *IEEE Trans. Inform. Theory*, vol. 49, pp. 707–720, Mar. 2003.

[19] Z. Wang, S. Zhou, and G. B. Giannakis, "Joint coding-precoding with low-complexity turbo decoding," *IEEE Trans. Wireless Commun.*, to be published.

[20] L. Wei and C. Schlegel, "Synchronization requirements for multiuser OFDM on satellite mobile and two-path Rayleigh fading channels," *IEEE Trans. Commun.*, vol. 43, pp. 887–895, Feb.–Apr. 1995.

[21] Y. Xin, Z. Wang, and G. B. Giannakis, "Space–time diversity systems based on linear constellation precoding," *IEEE Trans. Wireless Commun.*, vol. 2, pp. 294–309, Mar. 2003.

[22] N. Yee, J.-P. Linnartz, and G. Fettweis, "Multicarrier CDMA in indoor wireless radio networks," in *Proc. IEEE PIMRC*, Sept. 1993, pp. 109–113.

[23] S. Zhou, G. B. Giannakis, and C. Le Martret, "Chip-interleaved block spread code-division multiple access," *IEEE Trans. Commun.*, vol. 50, pp. 235–248, Feb. 2002.

[24] S. Zhou, G. B. Giannakis, and A. Swami, "Frequency-hopped generalized MC-CDMA for multipath and interference suppression," in *Proc. MILCOM Conf.*, vol. 2, Los Angeles, CA, Oct. 22–25, 2000, pp. 937–941.

[25] W. Y. Zou and Y. Wu, "COFDM: An overview," *IEEE Trans. Broadcast.*, vol. 41, pp. 1–8, Mar. 1995.

Pengfei Xia (S'03) received the B.S. and M.S. degrees in electrical engineering from the University of Science and Technology of China (USTC), Hefei, China, in 1997 and 2000 respectively. He is currently working toward the Ph.D. degree in the Department of Electrical and Computer Engineering at the University of Minnesota, Minneapolis.

His research interest lies in the area of signal processing and communications, including multiple-input multiple-output wireless communications, transceiver designs, adaptive modulations, multicarrier transmissions, space–time codes, and iterative decoding techniques.

Shengli Zhou (M'03) received the B.S. degree in 1995 and the M.Sc. degree in 1998, from the University of Science and Technology of China (USTC), Hefei, China, both in electrical engineering and information science. He received the Ph.D. degree in electrical engineering from the University of Minnesota, Minneapolis, in 2002.

He joined the Department of Electrical and Computer Engineering, University of Connecticut, Storrs, as an Assistant Professor in 2003. His research interests lie in the areas of communications and signal processing, including channel estimation and equalization, multiuser and multicarrier communications, space–time coding, adaptive modulation, and cross-layer designs.

Georgios B. Giannakis (S'84–M'86–SM'91–F'97) received the Diploma in electrical engineering from the National Technical University of Athens, Greece, in 1981. He received the MSc. degree in electrical engineering in 1983, M.Sc. degree in mathematics in 1986, and the Ph.D. degree in electrical engineering in 1986, from the University of Southern California (USC), Los Angeles.

His general interests span the areas of communications and signal processing, estimation and detection theory, time-series analysis, and system identification, subjects on which he has published more than 150 journal papers, 300 conference papers, and two edited books. Current research focuses on transmitter and receiver diversity techniques for single- and multiuser fading communication channels, comples-field and space–time coding, multicarrier, ultra-wideband wireless communication systems, cross-layer designs, and distributed sensor networks.

Dr. Giannakis is the corecipient of four Best Paper Awards from the IEEE Signal Processing (SP) Society (1992, 1998, 2000, and 2001). He also received the Society's Technical Achievement Award in 2000. He co-organized three IEEE-SP Workshops, and guest co-edited four special issues. He has served as Editor in Chief for the IEEE SIGNAL PROCESSING L ETTERS, as Associate Editor for the IEEE TRANSACTIONS ON SIGNAL PROCESSING and the IEEE SIGNAL PROCESSING LETTERS, as secretary of the SP Conference Board, as member of the SP Publications Board, as member and vice-chair of the Statistical Signal and Array Processing Technical Committee, and as chair of the SP for Communications Technical Committee. He is a member of the Editorial Board for the PROCEEDINGS OF THE IEEE, and the steering committee of the IEEE TRANSACTIONS ON WIRELESS COMMUNICATIONS. He is a member of the IEEE Fellows Election Committee, and the IEEE-SP Society's Board of Governors.